# Effect of Temperature on the Elastic Properties of Hydrogel: Modeling and AFM Experiments

Hansung Kim[1], Da Xu[1], Aditya B. Lingaraju[1], Harvey Abramowitz[1]

Department of Mechanical and Civil Engineering, Purdue University Northwest, Hammond, IN 46323, USA.

Corresponding author: kim886@purdue.edu

Hydrogel is getting significant attention as a biomedical material in the applications of tissue engineering and drug delivery. Since a hydrogel is a network of polymers containing significant amount of fluid, it shows a viscoelastic behavior and it's mechanical properties are influenced by temperature. In this research, we developed a modeling algorithm to predict the effect of temperature (T) on the Young's modulus (E) and stiffness of a commercial hydrogel using finite element method (FEM) complemented by Atomic Force Microscopy (AFM). In addition, we developed a quantative model describing the stiffness and Young's modulus of hydrogel as a function of temperature by adopting Arrhenius equation. Our FEM simulation results of force-displacement curves show a good agreement with AFM experimental data. Hertz contact theory was used to calculate the young's modulus of the hydrogel from the force-displacement curves of AFM at different temperatures ranging from 20°C to 50°C.

## I. Introduction

Hydrogels serve as important biomedical materials for drug delivery and tissue engineering because of their biocompatibility and mechanical properties.[1-3] Since a variety of biomedical applications employ hydrogels with various temperatures, it is necessary to measure temperature-dependent mechanical properties of hydrogels. Researchers have measured mechanical properties of hydrogels at the macro-scale as well as the micro/nano-scales.[4-6] At macro-scale, researchers commonly use universal testing machine and dynamic mechanical analysis (DMA) [1, 7] while indentation testing is commonly used to investigate the properties of hydrogel ranging from millimeter (mm) to nanometer (nm).[8, 9] Especially, Atomic Force Microscopy (AFM) is used for characterizing properties of hydrogel at nanoscale.[1, 4, 6] Temperature-dependent properties of hydrogel have been investigated by researchers. Hu et al. [10] investigate the temperature effect on the mechanical properties (Young's modulus and yielding parameters) of poly(N,N-dimethylacrylamide-co-methacrylic acid) hydrogels ranging 3°C to 37 °C based on using tensile tests. They found that chemical network dominates the mechanical properties at high temperature while strain-induced dissociation of hydrogen bond dominated the mechanical properties at lower temperature. Matzelle et al. [11] also investigated the temperature effect on the elastic modulus of poly(N-isopropylacrylamide) (PNIPAm) using AFM. They found out that the cross-linker concentration has a strong influence on Young's modulus for temperatures above the critical temperature while only small variations were seen for temperatures below the critical temperature for PNIPAm. There are multiple studies

investigating the behavior of hydrogel using finite element method (FEM) simulations. Mazaheri et al. [12] developed a constitutive model for PNIPAM hydrogels taking into account pH and temperature. They performed FEM simulation to predict homogeneous and inhomogeneous swelling behavior of PNIPAM hydrogels and showed a good agreement with experimental data. Li et al.[13] carried out FEM simulations of hydrogel-based contact lens to predict the force-displacement of the contact lens using an empirical viscoelastic model. They also compared FEM simulation results with micro-shaft-poking (MSP) experimental data. Tang et al.[14] investigated the micromechanical properties of hard sphere filled composite hydrogels using atomic force microscopy and finite element simulations. They constructed finite element model to simulate nanoindentation behaviors of AFM. Their main goal is to understand the effect of particles embedded in the hydrogel on the overall mechanical behaviors of composite hydrogel under indentation contact. They were able to develop quantitative relationship between particle size and elastic modulus of the overall composite. However, there are few studies on modeling temperature-dependent Young's modulus and stiffness of hydrogel at nanoscale utilizing finite element simulation and AFM experiments.

In this research, we developed a modeling algorithm to predict the Young's modulus and stiffness of a commercially available hydrogel as a function of temperature utilizing finite element simulation and AFM experiments. We were able to develop a quantitative model relating Young's modulus and stiffness of a hydrogel as a function of temperature utilizing Arrhenius equation.

## II. Experimental Procedure

The hydrogel used for our research is a commercial hydrogel pad for wound restoration fabricated by Ameda Company (Comfort Gel$^{TM}$). The hydrogel pad was cut into square (0.5 x 0.5 in) and placed on the sample plate of temperature-controlled AFM (Fig 1.). The AFM used for our research is TT-AFM by AFM Workshop company, which can generate force-displacement curves through indentation.

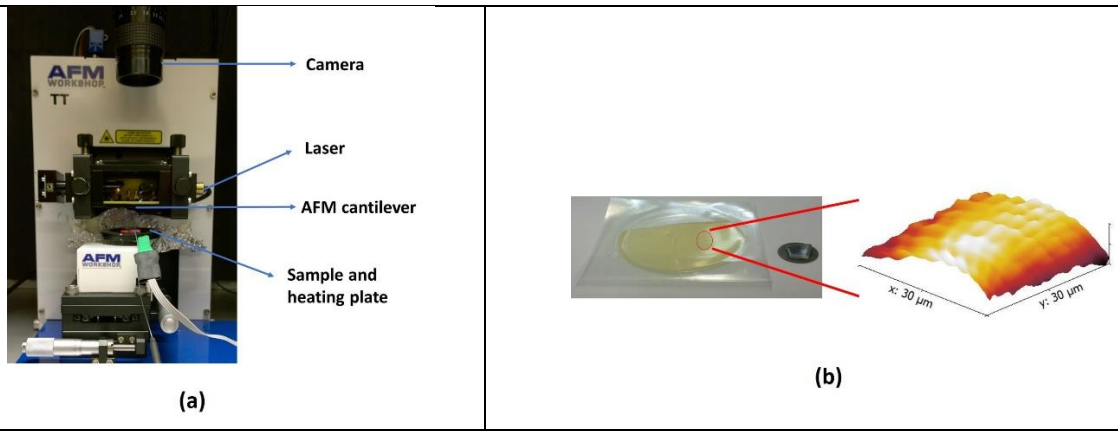


Fig 1. (a) AFM setup of hydrogel experiment (b) Hydrogel sample and AFM image of the hydrogel (30 x 30 µm)

# III. Modeling and Simulation Procedure

Hertz contact model was used to calculate Young's modulus from AFM force-displacement curve. The Hertz model is generally used for contact modeling where viscous contribution and deformation is small for biomaterials. Hertz model equation is shown as below

$$\mathrm{F} = \frac{4}{3} E^* \sqrt{R} d^{2/3} \quad (1)$$

$$E^* = \left[ \frac{1-v_{tip}^2}{E_{tip}} - \frac{1-v_{sample}^2}{E_{sample}} \right]^{-1} \quad (2)$$

R is the radius of the tip, E is the Young's modulus, $v$ is the Poisson's ratio and E* is the equivalent elastic modulus between the tip and the sample. The AFM tip is made of single crystal silicon. Mechanical properties of tip and hydrogel sample are described in Table 1. Since the Young's modulus and Poisson's ratio of single crystal silicon is dependent on the crystal direction, it is hard to obtain accurate values. Wortman and Evan calculated the Young's modulus and Poisson's ratio of single crystal silicon of (100) plane as a function of crystal orientation.[15] From their calculation, the Young's modulus of single crystal silicon of (100) plane varies from ~130 GPa to 165 GPA while the Poisson's ratio varies from ~0.06 to 0.28. So, we used average values ($E_{tip}$=150 GPa, $v_{tip}$= 0.17) of those ranges for contact model calculation as well as FEM simulations. The Poisson's ratio of hydrogel ranges between 0.36 – 0.5 based on published studies. [4, 5] We used average value of those range ($v_{sample}$ *=0.43)* for the Poisson's ratio of hydrogel for our modeling.

Table 1. Elastic and geometrical properties of tip and samples used in this study

| | $R$ (nm) | $v_{\mathrm{tip}}$ | $v_{sample}$ | $E_{tip}$ (GPa) |
|---|---|---|---|---|
| Magnitude | 10 | 0.17 | 0.43 | 150 |

COMSOL Multiphysics software is used for our FEM simulation. We performed FEM simulation with a 2D plane strain and axisymmetric assumption. AFM tip radius is 10nm and hydrogel dimension is 50 x 50 nm as illustrated in Fig 2(a). Mesh size of contact region is ~ 0.1nm while that of non-contact region gradually increases as moving away from the contact region, as shown in Fig 2(b).

For FEM simulation of tip indenting hydrogel, the tip is modeled as a linear elastic model. The hydrogel is modeled as linear elastic material model combined with Kevin-Voigt viscoelasticity. Kevin-Voight model is described as below

$$\sigma = E\varepsilon + \eta\dot{\varepsilon}$$

$$\eta = G\tau$$

σ : Stress, ε: Strain, $\dot{\varepsilon}$ : Strain rate, $\eta$ : Viscosity, $G$: Shear modulus, $\tau$ : Relaxation time

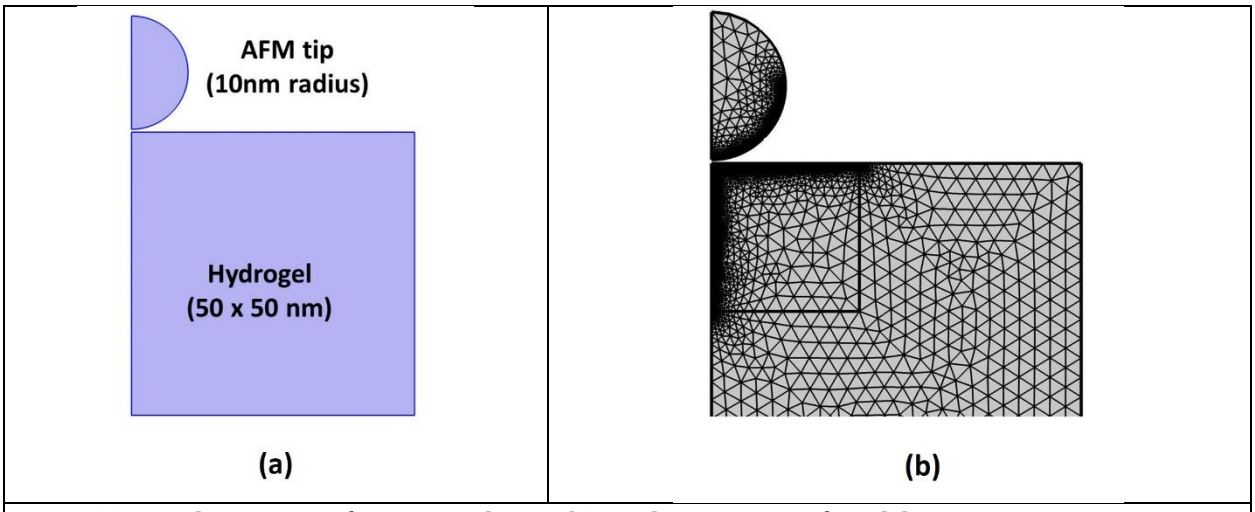


Fig 2. (a) Initial geometry of FEM simulation (b) Mesh generation of model

It is known that elastic properties (E and G) are not a strong function of temperature since elastic properties are mainly determined by chemical structure (chemical bonding). Therefore, relaxation time is considered as a main factor to control the temperature-dependent.

Since our AFM indentation is small and AFM data shows linear force-displacement curve, our obtained young's modulus is effective Young's modulus assuming linear elastic region as shown below

$$\sigma = E\varepsilon + \eta\dot{\varepsilon} = E_{effective}\varepsilon, \quad E_{effective} : \text{Effective young's modulus}$$

To predict the temperature dependent behavior of hydrogel, the relaxation time of the Kevin-Voigt model was optimized for each temperature by comparing the stiffness of force-displacement curve between AFM data and FEM simulation. More detail schematic of the optimization process is shown below.

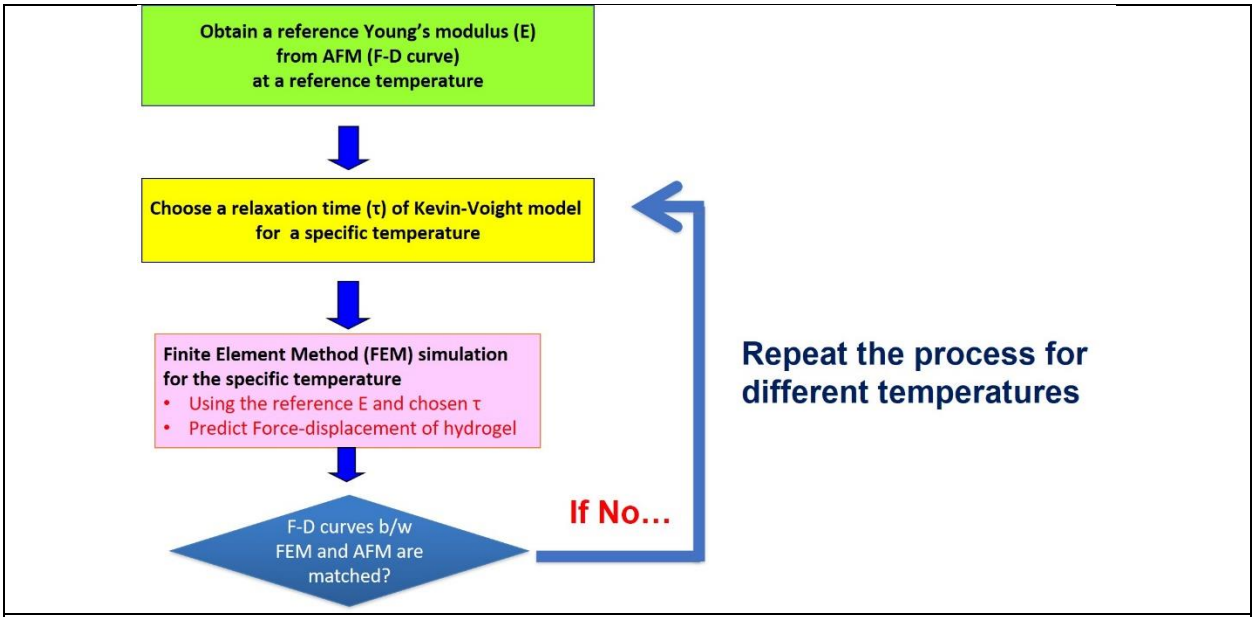


Fig 3. A schematic illustrating the procedure of optimizing relaxation time for FEM simulation

After Young's modulus of hydrogel was obtained as a function of temperature, we modeled the temperature dependent Young's modulus (E) using Arrhenius type equation as shown below,

$$E = Ae^{\frac{-E_a}{RT}}$$

$A$ : Coefficient, $T$: Absolute temperature (K), $R$: Universal gas constant, $E_a$: Activation energy

By plotting ln($E$) vs $\frac{1}{T}$ , the activation energy ($E_a$) cab be calculated from the slope and the coefficient A can be obtained from the intercept.

# IV. Results and Discussion

Fig 4. Shows the comparison of force-displacement curves between AFM experiment and FEM simulation. The experimental data of each temperature are average values of 3 different AFM measurements. Table 2 compares the stiffness of hydrogel from AFM experiment, the stiffness of hydrogel from FEM simulation, optimized relaxation time of Kevin-Voigt model for each temperature. Using the data of Table 2. the activation energy ($E_a$) and coefficient (A) of the Arrhenius equation were calculated for the Young's modulus and stiffness of hydrogel as described in Table 3.

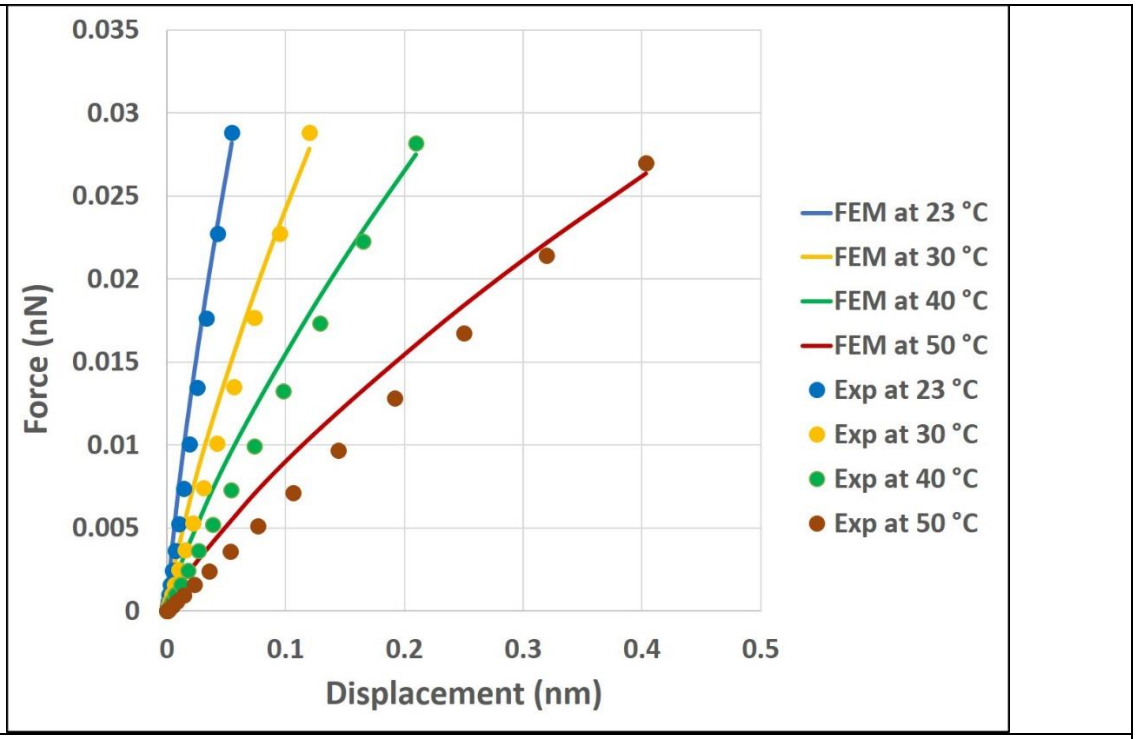


Fig 4. Comparison of force-displacement between FEM simulation and AFM experiments

Table 2. Comparison of the effective young's modulus of hydrogel from AFM experiment, the stiffness of hydrogel from FEM simulation, optimized relaxation time of Kevin-Voigt model for each temperature.

| Temperature | Young's modulus (MPa) | Stiffness (N/m) | Relaxation time (sec) |
|---|---|---|---|
| 23 °C | 5.25 | 0.53 | 532 |
| 30 °C | 2.33 | 0.24 | 237 |
| 40 °C | 1.27 | 0.13 | 133 |
| 50 °C | 0.66 | 0.067 | 65 |

The magnitudes of obtained Young's modulus are comparable to those of Drira and Yadavalli's study.[6] Their measured value of Young's modulus for polyethyleneglycol diacrylate (PEG-DA) hydrogel ranges mostly between 1-5 MPa, which is based on AFM indentation.

Fig 5. illustrate the Von Mises stress of FEM simulation when the tip indented into the hydrogel when the relaxation time of hydrogel is 65s. To acquire optimized relaxation time of hydrogel for each temperature, we used the Young's modulus of 23 °C (E = 5.25 GPa) as the reference Yong's modulus.

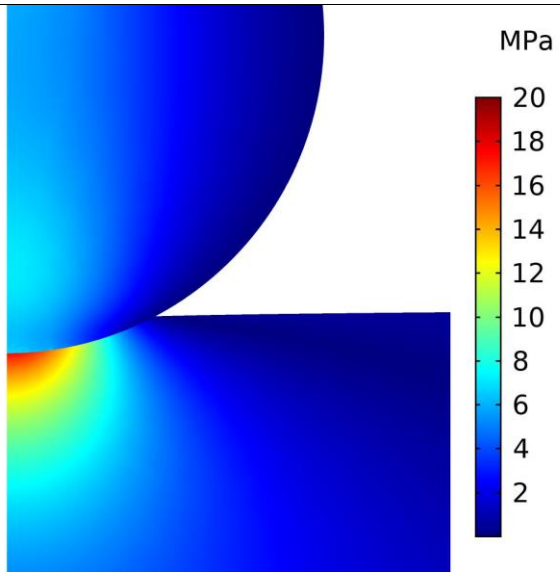


Fig 5. Von Mises stress of indentation between the tip and hydrogel

Table 3. The activation energy ($E_a$) and coefficient ($A$) of the Arrhenius equation for the Young's modulus and stiffness of hydrogel

| | Activation energy ($E_a$) | Coefficient ($A$) |
|---|---|---|
| Young's modulus (E) | -59204 (J/mol) | $e^{-22.5}$ |
| Stiffness (k) | -59146 (J/mol) | $e^{-24.8}$ |

From the data of Table 3, negative activation energy clarifies that Young's modulus decreases as the temperature increases. Moreover, it is noticed that the activation energy of Young's modulus is almost identical to that of stiffness, which verifies the capability of our contact model in preserving the chemistry of force-displacement reaction into Young's modulus. We also found that relaxation time of hydrogel also has similar activation energy as Young's modulus demonstrating the temperature-dependent Young's modulus of hydrogel is directly related the temperature-dependent relaxation time.

Fig 6. illustrates the ln (E) vs. (1/T) for Young's modulus and ln (k) vs. (1/T) for stiffness with linear trend lines verifying the legitimacy of Arrhenius model.

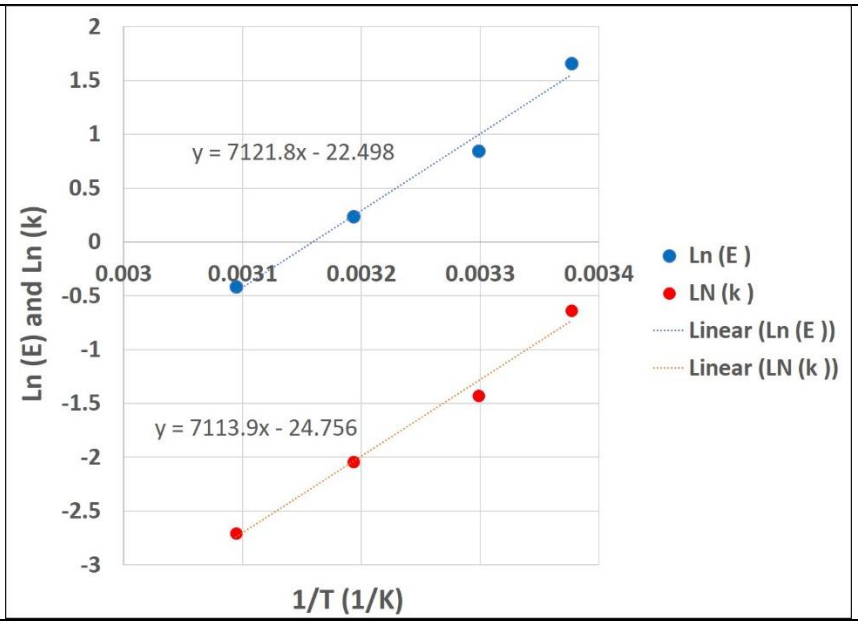


Fig 6. ln (E) vs. (1/T) for Young's modulus and ln (k) vs. (1/T) for stiffness with linear trend lines

# V. Conclusion

We developed the modeling algorithm to predict the Young's modulus and stiffness of a hydrogel utilizing Atomic Force microscopy (AFM), Finite Element Method (FEM) simulation, and Arrhenius equation. Through reverse engineering process based on AFM data and FEM simulation, optimum values of viscoelastic relaxation time of hydrogel were obtained for different temperatures. Using the optimized values of relaxation, the FEM simulation results show a good agreement with AFM experimental data. Through the analysis of Arrhenius equation of Young's modulus, stiffness, and relaxation time, we found that temperature-dependent Young's modulus of hydrogel is directly related to the relaxation time variation due to temperature.

# REFERENCES


1. M.L. Oyen, Int. Mater. Rev., 2014. 59(1): p. 44-59.
2. P. Gupta, K. Vermani, and S. Garg, Drug Discovery Today, 2002. 7(10): p. 569-579.
3. B. Baroli, J. Pharm. Sci., 2007. 96(9): p. 2197-2223.
4. C.D. Markert, X.Y. Guo, A. Skardal, Z. Wang, S. Bharadwaj, Y.Y. Zhang, K. Bonin, and M. Guthold, J. Mech. Behav. Biomed. Mater., 2013. 27: p. 115-127.
5. U. Chippada, B. Yurke, and N.A. Langrana, J. Mater. Res., 2010. 25(3): p. 545-555.
6. Z. Drira and V.K. Yadavalli, J. Mech. Behav. Biomed. Mater., 2013. 18: p. 20-28.
7. R. Kocen, M. Gasik, A. Gantar, and S. Novak, Biomed. Mater., 2017. 12(2).
8. M. Galli, K.S.C. Comley, T.A.V. Shean, and M.L. Oyen, J. Mater. Res., 2009. 24(3): p. 973-979.
9. L. Qian and H.W. Zhao, Micromachines, 2018. 9(12).
10. X.B. Hu, J. Zhou, W.F.M. Daniel, M. Vatankhah-Varnoosfaderani, A.V. Dobrynin, and S.S. Sheiko, Macromolecules, 2017. 50(2): p. 652-659.
11. T.R. Matzelle, G. Geuskens, and N. Kruse, Macromolecules, 2003. 36(8): p. 2926-2931.
12. H. Mazaheri, M. Baghani, R. Naghdabadi, and S. Sohrabpour, Smart Mater. Struct., 2016. 25(8).
13. C. Li, M. Ahearne, and K.K. Liu, Int. J. Mod. Phys. B, 2010. 24(1-2): p. 117-127.
14. G.L. Tang, M. Galluzzi, C.S. Biswas, and F.J. Stadler, J. Mech. Behav. Biomed. Mater., 2018. 78: p. 496-504.
15. J.J. Wortman and R.A. Evans, J. Appl. Phys., 1965, 153-156.